

Tunable absorption coefficient in GaAs doping superlattices

G. H. Döhler, H. Künzel, and K. Ploog

*Max-Planck-Institut für Festkörperforschung, Heisenbergstrasse 1,
D-7000 Stuttgart 80, Federal Republic of Germany*

(Received 18 August 1981)

The optical-absorption coefficient $\alpha(\omega)$ of GaAs "NIPI" crystals [a new type of semiconductor superlattice consisting of n - and p -doped layers, possibly separated by intrinsic (i) regions, in an otherwise homogeneous bulk] is measured at photon energies below the forbidden gap of the unmodulated material. We use the extremely strong photoconductive response of these NIPI crystals as a very sensitive method for the detection of very weak absorption signals in the tail far below the gap of bulk GaAs. Another peculiarity of NIPI crystals expected from theory is the tunability of $\alpha(\omega)$ by variation of the energy gap, which is no longer a constant quantity for these systems. The experimental results on molecular-beam-epitaxy-grown GaAs NIPI crystals reported in this paper show that both the frequency dependence and the dependence on modulation of the band gap are in excellent agreement with theory.

INTRODUCTION

Semiconductor superlattices with a periodic variation of alloy composition on a scale of a few $10-10^2$ Å with GaAs and $\text{Al}_x\text{Ga}_{1-x}\text{As}$ and, more recently, InAs and GaSb as the constituents, have been the subject of intense experimental and theoretical studies.^{1,2} In contrast to these "compositional superlattices" another class of semiconductor superlattices, consisting of a homogeneous bulk material only modulated by periodic n and p doping, had not been investigated experimentally until recently,^{3,4} although many intriguing electronic and optical properties had been predicted quite some time ago for these np -doping superlattices (also called "NIPI" crystals⁵⁻⁷). The most striking features of np -doping superstructures with respect to the present investigation are the following:

- (1) They have an "indirect gap in real space" since the lowest conduction-band states are shifted by half a superlattice spacing with respect to the uppermost valence-band states.
- (2) Electron-hole recombination lifetimes may exceed the corresponding values of unmodulated bulk material by many orders of magnitude because of a small spatial overlap of electron and hole states. This feature allows large deviations of electron and hole concentration from equilibrium values even at extremely low excitation intensities.
- (3) The varying space charge associated with a variable electron and hole concentration induces strong changes of the effective energy gap E_g^{NIPI} , which is always smaller than the gap of the un-

modulated semiconductor material E_g^0 .

The optical absorption $\alpha(\omega)$ at photon energies $\hbar\omega$ slightly above the effective energy gap E_g^{NIPI} is expected to be extremely low because of the small overlap between the conduction- and valence-band states involved in this process. With increasing photon energy, $\alpha(\omega)$ increases exponentially and finally becomes comparable with typical bulk values at $\hbar\omega \gtrsim E_g^0$. The behavior of $\alpha(\omega)$ for photon energies $\hbar\omega < E_g^0$ is of particular interest since $\alpha(\omega)$ is no longer a constant quantity for NIPI crystals. $\alpha(\omega)$ varies over a wide range if the energy gap is modulated by changing the carrier concentration.

Measurements of extremely weak absorption coefficients are possible in NIPI crystals by an analysis of the strong photoconductive response. Owing to the very long recombination lifetime the concentration of photogenerated electrons and holes increases with the absorbed dose.⁸ The photoresponse saturates only when the electron-hole generation rate becomes comparable with the (very low) recombination rate. Thus, the time dependence of the photoconductivity is directly related to $\alpha(\omega)$, and $\alpha(\omega)$ may be determined from photoconductivity versus time measurements.

In the first section of this paper we will briefly discuss the electronic structure of a doping superlattice for the quasicontinuum limit corresponding to rather large superlattice periods, as investigated experimentally in the present study. Then we will derive the expressions for the absorption coefficient $\alpha(\omega)$ as well as for the photoconductive response.

In Sec. II the sample preparation by molecular-

beam epitaxy and the experimental procedure of absorption measurements will be described. The experimental results will then be compared with the theoretical predictions from the first section. In our concluding remarks we will stress some related projects and we will also discuss implications for future applications.

I. THEORY

A. Electronic structure of a doping superlattice with long period

We consider the case of a periodic structure composed of homogeneously doped n and p layers of thickness d_n and d_p and donor concentrations n_D and acceptor concentrations n_A , respectively, with intrinsic layers of thickness d_i in between (see Fig. 1).

The following approximations are made for the calculation of the periodic space-charge potential in the crystal:

(1) Any subband effects resulting from the quantization of the motion in the direction of periodicity may be neglected, if the layers are sufficiently thick.

(2) Instead of calculating the space-charge distribution self-consistently⁹ we assume that the impurity space charge is exactly neutralized in the central regions of width d_n^0 and d_p^0 in the respective layers by free carriers, whereas the impurity space charge is uncompensated in the remaining fractions of the doping layers of width

$$2d_n^+ = d_n - d_n^0 \quad (1)$$

and

$$2d_p^- = d_p - d_p^0, \quad (2)$$

respectively.

The (two-dimensional) density of electrons per n layer and of holes per p layer is

$$n^{(2)} = n_D d_n^0 \quad (3)$$

and

$$p^{(2)} = n_A d_p^0, \quad (4)$$

respectively. The condition of macroscopic neutrality requires that

$$v(z)L = \begin{cases} (2\pi e^2 n_D / \epsilon) (|z| - d_n^0/2)^2 & \text{for } d_n^0/2 < |z| < d_n/2 \\ 2\Delta V - (2\pi e^2 n_A / \epsilon) (|z| - (d - d_p^0)/2)^2 & \text{for } (d - d_p^0)/2 < |z| < (d - d_p^0)/2, \end{cases} \quad (9)$$

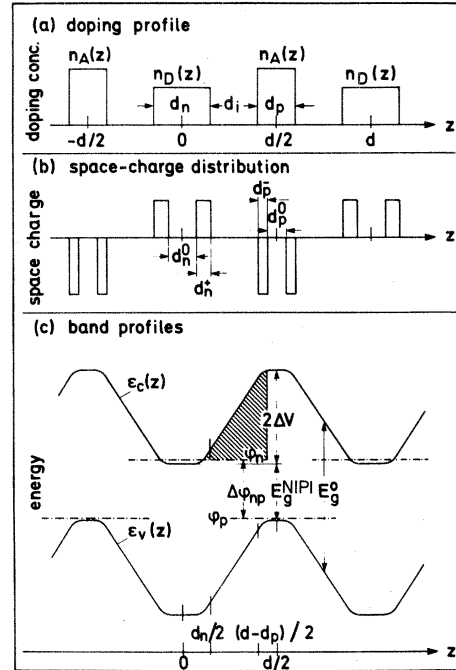


FIG. 1. Schematic diagram of (a) doping profile, (b) space-charge distribution, and (c) band profiles in periodic NIPI doping structures at given layer thicknesses d_n , d_p , and d_i and doping concentrations n_D , n_A , and $n_i=0$ in the n and p doped and intrinsic layers, respectively. Quantum effects are neglected. The effective energy gap E_g^{NIPI} is reduced by the amount of $2\Delta V$ compared to the unmodulated bulk value E_g^0 due to the periodic space-charge potential. The difference between electron and hole quasi-Fermi-levels $\Delta\phi_{np}$ corresponds approximately to E_g^{NIPI} as long as there are neutral regions of finite width d_n^0 and d_p^0 in the doping layers.

$$n_D d_n^+ = n_A d_p^-, \quad (5)$$

which yields a relation between $n^{(2)}$ and $p^{(2)}$:

$$n^{(2)} = p^{(2)} + n_D d_n - n_A d_p. \quad (6)$$

The periodic space-charge potential $v(z)$ for $-d/2 < z < d/2$ is then

(1) constant in the neutral part of the doping layers, i.e.,

$$v(z) = \begin{cases} 0 & \text{for } |z| < d_n^0/2 \\ 2\Delta V & \text{for } (d - d_p^0)/2 < |z| < d/2, \end{cases} \quad (7)$$

(2) parabolic in the ionized impurity regions, i.e.,

$$v(z) = \begin{cases} (2\pi e^2 n_D / \epsilon) (|z| - d_n^0/2)^2 & \text{for } d_n^0/2 < |z| < d_n/2 \\ 2\Delta V - (2\pi e^2 n_A / \epsilon) (|z| - (d - d_p^0)/2)^2 & \text{for } (d - d_p^0)/2 < |z| < (d - d_p^0)/2, \end{cases} \quad (10)$$

(3) linearly increasing in the intrinsic layers (if present at all), i.e.,

$$v(z) = (4\pi e^2 n_D d_n^+) (d_n^+ / 2 + |z| - d_n / 2) / \epsilon \quad \text{for } d_n / 2 < |z| < (d - d_p) / 2. \quad (11)$$

ϵ is the static dielectric constant of the semiconductor. The amplitude ΔV of the space-charge potential is given by

$$2\Delta V = v(d/2) - v(0) = (4\pi e^2 / \epsilon) [n_D (d_n^+)^2 + n_A (d_p^-)^2 / 2 + n_D d_n^+ d_i]. \quad (12)$$

The potential $v(z)$ is modulating the conduction and the valence bands (see Fig. 1). For the band edges one has

$$\epsilon_c(z) = E_c + v(z) \quad (13)$$

and

$$\epsilon_v(z) = E_v + v(z), \quad (14)$$

with

$$E_c = E_v + E_g^0. \quad (15)$$

Therefore, the effective energy gap E_g^{NIPi} of the doping superlattice, i.e., the energy difference between the lowest electron states in conduction bands and the uppermost hole states in valence bands, is smaller by $2\Delta V$ compared with the unmodulated bulk value E_g^0 :

$$E_g^{\text{NIPi}} = \epsilon_c(z=0) - \epsilon_v(z=d/2) = E_g^0 - 2\Delta V. \quad (16)$$

The position of the Fermi level for the electrons relative to the conduction-band edge in the flat portions of the periodic potential is given by the corresponding bulk value for doping concentration n_D and the temperature T within our approximations:

$$\epsilon_c(z=0) - \phi_n = (E_c - \phi)_{n_D; T}. \quad (17)$$

A corresponding expression applies for the hole Fermi level ϕ_p :

$$\phi_p - \epsilon_v(z=d/2) = (\phi - E_v)_{n_A; T}. \quad (18)$$

Although the condition for thermal equilibrium requires $\phi_n = \phi_p$, a nonequilibrium situation with $\phi_n \neq \phi_p$ may be quasistable. If, for instance, the system is in a state with $\phi_n < \phi_p$, as shown in Fig. 1, it can return to equilibrium only by electron-hole recombination, either by thermal activation over the potential barrier or by tunneling through it. Both processes, however, have extremely small

probabilities if the heights ($\sim 2\Delta V$) and the width of the barrier (see shaded area in Fig. 1) are sufficiently large. The expressions (1)–(6) and (12)–(16) relate the carrier concentrations $n^{(2)}$ and $p^{(2)}$ to the effective gap E_g^{NIPi} and, by (17) and (18) with the quasi-Fermi-level difference,

$$\Delta\phi_{np} = \phi_n - \phi_p. \quad (19)$$

Later on the values of $n^{(2)}$ and $p^{(2)}$ as a function of $\Delta\phi_{np}$ will be needed. For these quantities one obtains

$$n^{(2)} = n_D d_n - n_0^{(2)} \left[\left(1 + \frac{V_{bi} - \Delta\phi_{np}}{(2\Delta V)_0} \right)^{1/2} - 1 \right] \quad (20)$$

and

$$p^{(2)} = n_A d_p - n_0^{(2)} \left[\left(1 + \frac{V_{bi} - \Delta\phi_{np}}{(2\Delta V)_0} \right)^{1/2} - 1 \right], \quad (21)$$

with

$$n_0^{(2)} = [n_A n_D / (n_A + n_D)] d_i, \quad (22)$$

$$(2\Delta V)_0 = (2\pi e^2 / \epsilon) n_0^{(2)} d_i, \quad (23)$$

and

$$V_{bi} = E_g - (E_c - \phi)_n - (\phi - E_v)_p. \quad (24)$$

As the carrier concentrations may never become negative, a minimum value of the quasi-Fermi-level difference $\Delta\phi_{np}^{\text{th}}$ can be calculated from the threshold condition that the "minority layer" is totally depleted. The expressions (20) and (21) yield

$$n_0^{(2)} \left[\left(1 + \frac{V_{bi} - \Delta\phi_{np}^{\text{th}}}{(2\Delta V)_0} \right)^{1/2} - 1 \right] = \min\{ n_D d_n, n_A d_p \}, \quad (25)$$

whence¹⁰

$$\Delta\phi_{np}^{\text{th}} = V_{bi} - (2\Delta V) \times \left\{ \left[\left(1 + \left[1 + \frac{n_A}{n_D} \right] \frac{d_p}{d_i} \right)^2 - 1 \right] \right\}, \quad n_D d_n > n_A d_p \quad (26)$$

$$\left\{ \left[\left(1 + \left[1 + \frac{n_D}{n_A} \right] \frac{d_n}{d_i} \right)^2 - 1 \right] \right\}, \quad n_D d_n < n_A d_p. \quad (27)$$

It should be noted that the condition of macroscopic charge neutrality also requires that the carrier concentration in the "majority layers" may not be reduced below its value at $\Delta\phi_{np}^{\text{th}}$, i.e.,

$$n_{\text{min}}^{(2)} = n_D d_n - n_A d_p \quad \text{if } n_D d_n > n_A d_p \quad (28)$$

or

$$p_{\text{min}}^{(2)} = n_A d_p - n_D d_n \quad \text{if } n_A d_p > n_D d_n. \quad (29)$$

The value of $\Delta\phi_{np}^{\text{th}}$ may be positive or negative, depending on the design parameters n_D , n_A , d_n , d_p , and d_i . Because of $\Delta\phi_{np} \approx E_g^{\text{NIPI}}$, negative values of $\Delta\phi_{np}^{\text{th}}$ imply the possibility of having negative effective gaps. If $\Delta\phi_{np}^{\text{th}} > 0$ the minority layers will be depleted in the ground state of the system. If, however, $\Delta\phi_{np}^{\text{th}} < 0$ there will be a finite carrier concentration in both types of layers at thermal equilibrium, which is obtained from (20) and (21) with $\Delta\phi_{np} = 0$.

B. Theory of optical absorption in NIPI crystals—continuum limit

Optical absorption in a NIPI crystal, in principle, is possible once the photon energy $\hbar\omega$ exceeds the effective energy gap E_g^{NIPI} (or, more accurately, for the case of finite $n^{(2)}$ and $p^{(2)}$, if $\hbar\omega > \Delta\phi_{np}$). In practice, however, the interband matrix elements for transitions between the uppermost valence and the lowest conduction subbands are extremely small for the case of large superlattice period and moderate doping concentration, as used in the experiments described below. The matrix elements, however, increase exponentially as $\hbar\omega$ approaches the gap of the unmodulated bulk E_g^0 . Consequently, an exponential increase of the absorption coefficient with $\hbar\omega$ is expected and values comparable with the unmodulated bulk are expected in the photon-energy range above E_g^0 .

It is also clear from the very beginning that the absorption coefficient of a NIPI crystal as a function of photon energy $\alpha^{\text{NIPI}}(\omega)$ will be a function of the effective energy gap E_g^{NIPI} and, therefore, of the quasi-Fermi-level difference $\Delta\phi_{np}$, since the optical matrix elements will be strongly influenced by variations of the periodic space-charge potential. A detailed theoretical study of $\alpha^{\text{NIPI}}(\omega; \Delta\phi_{np})$, in which oscillations due to the discrete subband structure will be considered, is deferred to another publication.¹¹ Quantum oscillations are not expected to be observable in the structures, which are the subject of the present investigation because of too

large superlattice periods. For our problem a continuum approach will represent a sufficiently good approximation as the spatial variation of the internal fields,

$$eF_i(z) = \left[\frac{dv}{dz} \right]_z, \quad (30)$$

is rather slow and the envelope wave functions of the true subbands do not differ significantly from the Airy functions obtained for homogeneous fields near the band edges (see Fig. 2).

The absorption coefficient of a NIPI crystal $\alpha^{\text{NIPI}}(\omega; \Delta\phi_{np})$ in this continuum approximation is given by the bulk value $\alpha^b(\omega; F_i)$ averaged over the internal local-field distribution. Thus, one has

$$\alpha^{\text{NIPI}}(\omega; \Delta\phi_{np}) \approx d^{-1} \int_0^d dz \alpha^b(\omega; F_i(z)). \quad (31)$$

The shape of $F_i(z)$ follows directly from the expressions (7)–(11) for $v(z)$ by differentiation. For the case of constant doping in the n and p layers, $F_i(z)$ increases and decreases linearly from zero to its maximum value in the ionized impurity regions, whence one obtains

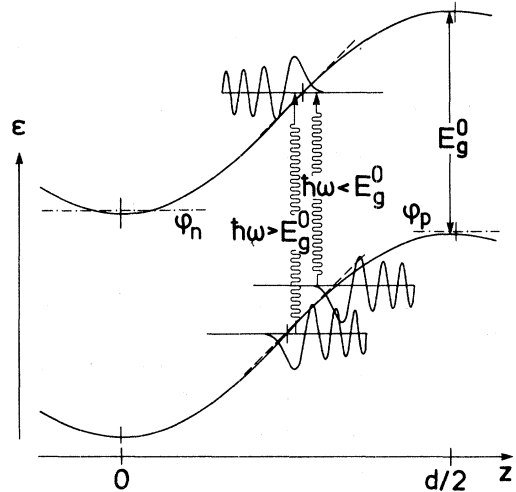


FIG. 2. Illustration of the continuum approach used for calculating the absorption coefficient in NIPI crystals with large period. The errors introduced by the approximation contained in the expressions (31) and (32) are negligible if the gradient of the space-charge potential remains roughly constant (indicated by dashed-straight lines) in the overlap region of valence- and conduction-band states differing in energy by $\hbar\omega$. For the design parameters of the investigated samples the decay in z direction beyond the classical turning point and the oscillation period of the Airy functions at positive kinetic energies is much shorter than depicted in the figure.

$$\alpha^{\text{NIPI}}(\omega; \Delta\phi_{np}) \approx d^{-1} \left[d_n^0 \alpha_n^b(\omega) + d_p^0 \alpha_p^b(\omega) + 2d_i \alpha^b(\omega; F_{i,\max}) + 2(d_n^+ + d_p^- F_{i,\max}) \int_0^{F_{i,\max}} dF \alpha^b(\omega; F) \right]_{\Delta\phi_{np}}. \quad (32)$$

The subscript on the right-hand side of (32) should be a reminder that for the quantities d_n^0 , d_p^0 , d_n^+ , d_p^- , and $F_{i,\max}$ their respective values at $\Delta\phi_{np}$ should be taken. $\alpha_n^b(\omega)$ and $\alpha_p^b(\omega)$ are the absorption coefficients of an unmodulated n - and p -type bulk material of the corresponding doping strength at zero electric field.

The finite absorption for $\hbar\omega < E_g^0$ in a bulk under the influence of a homogeneous electric field is due to the Franz-Keldysh effect.¹² For our calculation of $\alpha^b(\omega; F)$ we use the analytical expression as obtained for the effective-mass approximation,¹³ assuming isotropic bands.

The imaginary part of the dielectric function at an electric field F is then given by

$$\epsilon_2(\omega; F) = C \sum_i \mu_i^{3/2} (\hbar\Omega_i)^{1/2} \times \int_0^\infty dx x^{1/2} \text{Ai}(x + x_{0,i}), \quad (33)$$

where

$$\hbar\Omega_i = 2^{-2/3} [(\hbar^2/2)(e^2 F^2 / \mu_i)]^{1/3} \quad (34)$$

is a characteristic energy for the electric field,

$$x_{0,i} = (E_g^0 - \hbar\omega) / \hbar\Omega_i, \quad (35)$$

and

$$\mu_i^{-1} = m_e^{-1} + m_{vi}^{-1} \quad (36)$$

is the reduced effective mass for transitions from the i th valence band into the conduction band. For photon energies $\hbar\omega$ below and close to the fundamental gap E_g^0 , it is sufficient to sum over heavy- and light-hole contributions only and to neglect the spin split-off band. In the effective-mass approximation $\epsilon_2(\omega; F)$ from (33) is related to the corresponding result for the field-free case in a simple way:

$$\epsilon_2(\omega; 0) = C \sum_i \mu_i^{3/2} (\hbar\omega - E_g^0)^{1/2} \Theta(\hbar\omega - E_g^0), \quad (37)$$

with

$$\Theta(\hbar\omega - E_g^0) = \begin{cases} 0 & \text{for } \hbar\omega < E_g^0 \\ 1 & \text{for } \hbar\omega > E_g^0 \end{cases} \quad (38)$$

and with the same constant C as in (33).

$\epsilon_2(\omega; F)$ increases exponentially for $\hbar\omega$ below E_g^0

and oscillates around $\epsilon_2(\omega; 0)$ above E_g^0 (Ref. 13) with a period of the order of $\hbar\Omega_i$, which is related to oscillations of the overlap between the conduction- and valence-band envelope functions as a function of $\hbar\omega$ (see Fig. 2). At higher photon energies $\epsilon_2(\omega; F)$ approaches $\epsilon_2(\omega; 0)$. The absorption coefficient is obtained by multiplication of ϵ_2 by ω / nc ,

$$\alpha(\omega) = (\omega / nc) \epsilon_2(\omega), \quad (39)$$

where n is the refraction index and c the velocity of light.

The integral in (32) may be evaluated numerically. The oscillations of $\alpha^b(\omega; F) / \alpha^b(\omega; 0)$ disappear in this contribution to $\alpha^{\text{NIPI}}(\omega; \Delta\phi_{np})$ by the field-averaging procedure. Therefore, $\alpha^{\text{NIPI}}(\omega; \Delta\phi_{np}) / \alpha^b(\omega; 0)$ will exhibit no oscillations at all if there are no intrinsic layers in the crystal. On the other hand, the oscillations will be most pronounced in a NIPI crystal with thin, strongly doped layers separated by relatively thick intrinsic layers, as the contribution $(2d_i/d)\alpha^b(\omega; F_{i,\max})$ will represent the dominant contribution to $\alpha^{\text{NIPI}}(\omega; \Delta\phi_{np})$.

In order to demonstrate the dependence of $\alpha^{\text{NIPI}}(\omega; \Delta\phi_{np})$ on the doping profile, the results of a numerical evaluation of (32) for the above-mentioned extreme cases are shown in Figs. 3 and

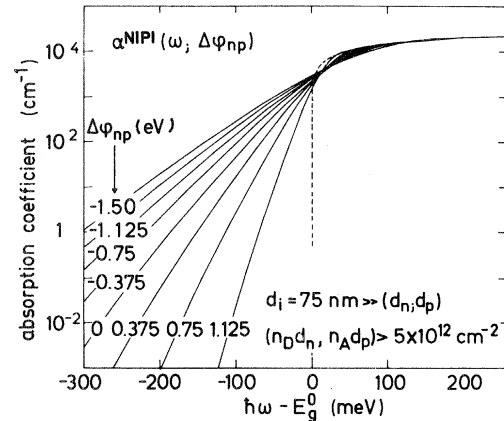


FIG. 3. Example 1: Calculated absorption coefficient of a NIPI crystal with dopants confined to very thin n and p layers separated by relatively thick intrinsic regions for various values of quasi-Fermi-level difference $\Delta\phi_{np}$. Internal space-charge field at $\Delta\phi_{np} = 0$ is 2×10^5 V cm⁻¹. (The dashed line indicates the absorption coefficient in pure homogeneous GaAs bulk material.)

4, respectively.¹⁴ In both cases the maximum field at $\Delta\phi_{np}=0$ is the same, $F_{i,\max}=2\times 10^5$ V cm⁻¹. It is obvious that the crystal with $(d_n;d_p)\ll d_i$ differs from the pure np -doping system by a more pronounced tunability.

C. Measurement of $\alpha^{\text{NIPI}}(\omega;\Delta\phi_{np})$ by photoconductive response

The absorption coefficient $\alpha^{\text{NIPI}}(\omega;\Delta\phi_{np})$ may be determined in the conventional way from the attenuation of the transmitted light as a function of ω for various values of $\Delta\phi_{np}$. The variation of $\Delta\phi_{np}$ can be achieved by an external potential eU_{np} applied via selective electrodes to the n and p layers, respectively.^{3,4,6,7} In this case electrons and holes are injected into or extracted from the NIPI crystal until the carrier concentrations $n^{(2)}$ and $p^{(2)}$ correspond to a quasi-Fermi-level difference $\Delta\phi_{np}=eU_{np}$ according to (20) and (21).

Another possibility of modulating $\Delta\phi_{np}$ is by absorption induced changes of $n^{(2)}$ and $p^{(2)}$.^{6,7} The electrons and holes generated by the absorption process are relaxing very fast down to the lower conduction or up to the upper valence-band edge, respectively. The recombination lifetime of the relaxed carriers, however, is very long because of small overlap between the respective electron and hole wave functions. The change of electron and hole concentration per layer with time $\dot{n}^{(2)}=\dot{p}^{(2)}$ is

given as the difference between the rate of electron-hole pairs generated by the absorption of $(I_\omega/\hbar\omega)\alpha(\omega;\Delta\phi_{np})d$ photons per layer (I_ω is the light intensity in the sample) and the rate of electron-hole recombination

$$\dot{n}^{(2)}=\dot{p}^{(2)}=(I_\omega/\hbar\omega)\alpha(\omega;\Delta\phi_{np})d-R(\Delta\phi_{np}). \quad (40)$$

The recombination rate $R(\Delta\phi_{np})$ is also a function of $\Delta\phi_{np}$. It increases with $\Delta\phi_{np}$ because of increasing overlap between relaxed electron and hole states. This increase of recombination rate is in contrast to the behavior of $\alpha(\omega < E_g^0/\hbar;\Delta\phi_{np})$. The absorption coefficient decreases since the overlap between valence- and conduction-band states differing in energy by $\hbar\omega < E_g^0$ decreases when the periodic potential becomes flatter due to increasing $\Delta\phi_{np}$ (see Fig. 2).

The differential equation (40), together with the relations (20) and (21) between the carrier concentrations $n^{(2)}$, $p^{(2)}$, and the Fermi-level difference $\Delta\phi_{np}$, describes the modulation of $\Delta\phi_{np}$ by light. The modulation of $\Delta\phi_{np}$ by light, however, does not only represent another possibility of varying the absorption coefficient. It also provides the basis for a very sensitive method for measurements of extremely low absorption coefficients in thin samples, or for the detection of low-intensity radiation. This will be described in the following.

Inspection of (40) tells us that the variation of carrier concentration with time is significantly influenced by the absorption of light as long as the recombination rate $R(\Delta\phi_{np})$ does not strongly exceed the rate of carrier generation by absorption of photons. The lifetime of excess carriers in NIPI crystals, however, is increased by many orders of magnitude as compared to an unmodulated bulk semiconductor (typically $\tau^{\text{NIPI}}\gg 1$ sec, if $\Delta\phi_{np}$ is not too large). Consequently, a photoresponse on the carrier concentration may still be detectable in a NIPI crystal, even if the photon absorption rate is reduced by many orders of magnitude compared with a bulk semiconductor. The light-induced changes of the carrier concentration may be measured as a variation of the photovoltage $eU_{np}=\Delta\phi_{np}$. This, however, is not the most appropriate and sensitive method in the case of small-absorption signals. If, instead of the photovoltage, the photoconductive response associated with the change of carrier concentration is used for the detection of the absorbed photons, no sensitive high-impedance voltage measurement has to be performed, but only changes of conductivity in the range of values typical for moderately to highly

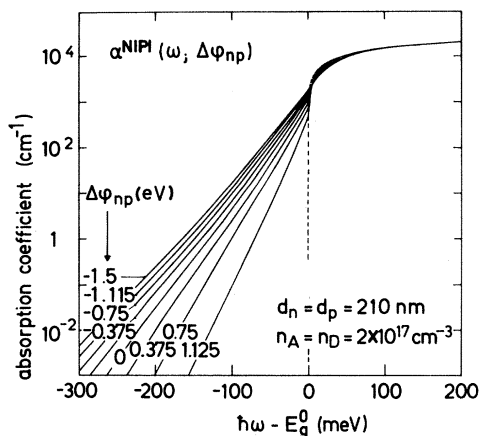


FIG. 4. Example 2: Calculated absorption coefficient of a NIPI crystal with uniformly doped n and p layers without intrinsic regions in between for various values of quasi-Fermi-level difference $\Delta\phi_{np}$. Maximum space-charge field at $\Delta\phi_{np}=0$ is 2×10^5 V cm⁻¹, as in example 1. (The dashed line indicates the absorption coefficient in pure homogeneous GaAs bulk material.)

doped semiconductors are to be measured. The photoconductive response of a NIPI crystal may be detected either as an increase of the electron conductivity $\sigma_{nn}^{(2)}(\Delta\phi_{np})$ in the n layers or as an increase of the hole conductivity $\sigma_{pp}^{(2)}(\Delta\phi_{np})$ in the p layers. These two conductivities and their variation can be measured independently with appropriate selective electrodes to the respective type of layers.⁴ For samples with the design as investigated in the present study it is a good approximation to assume

$$\sigma_{nn}^{(2)}(\Delta\phi_{np}) = e\mu_n n^{(2)}(\Delta\phi_{np}) \quad (41)$$

and

$$\sigma_{pp}^{(2)}(\Delta\phi_{np}) = e\mu_p p^{(2)}(\Delta\phi_{np}), \quad (42)$$

with constant values of the electron and hole mobilities μ_n and μ_p . This assumption is justified by the fact that $n^{(2)}$ and $p^{(2)}$ may be considered as the carrier concentration in a bulk semiconductor layer of thickness d_n^0 , or d_p^0 and with doping concentration n_D or n_A , respectively.

In Refs. 4 and 16 it is shown that (41) and (42) are indeed valid for the samples investigated in the present study. Moreover, it was verified that $n^{(2)}(\Delta\phi_{np})$ and $p^{(2)}(\Delta\phi_{np})$ as determined from experiment agrees with the calculated carrier-concentration versus Fermi-level difference relation according to (20) and (21).

Under these circumstances it is particularly easy to determine $\alpha(\omega; \Delta\phi_{np})$ from an observation of $\sigma_{nn}(t)$ or $\sigma_{pp}(t)$ at a given light intensity and fre-

quency I_ω . The recombination rate $R(\Delta\phi_{np})$ may be determined from the decay of the photoresponse at $I_\omega=0$ or it may be eliminated by subtracting the result obtained at two different values of I_ω . After converting $\sigma_{nn}^{(2)}(t)$ or $\sigma_{pp}^{(2)}(t)$ into $n^{(2)}(t)$ or $p^{(2)}(t)$ the absorption coefficient $\alpha(\omega; \Delta\phi_{np})$ is obtained with Eq. (40) from the time derivative of these curves at the ordinates $n^{(2)}$ or $p^{(2)}$, which corresponds to the desired value of $\Delta\phi_{np}$ given by (20) and (21).

Two remarks remain to be made.

(1) The analysis provides the exact values of $\alpha(\omega; \Delta\phi_{np})$ if the intensity incident onto the samples is known, including the reflection coefficient and if the quantum efficiency is unity. The latter assumption is a reasonable one since the relaxation processes of the photogenerated carriers are very fast compared with the recombination processes. There is also experimental evidence for this assumption from luminescence measurements.¹⁵ Radiative recombination is only observed between relaxed carriers at photon energies $\hbar\omega \approx \Delta\phi_{np} < E_g^0$, even when the photon energy of the absorbed light is considerably above the unmodulated gap value E_g^0 .

The expression for the absorption term in (40) is no longer correct when α or the thickness L_z of the crystal become so large that

$$\alpha L_z \ll 1 \quad (43)$$

is no longer fulfilled. In this case Eq. (40) has to be replaced by

$$n^{(2)} = p^{(2)} = I_\omega^0 / \hbar\omega \{ 1 - \exp[-\alpha^{\text{NIPI}}(\omega; \Delta\phi_{np}) L_z] \} d / L_z - R(\Delta\phi_{np}). \quad (40')$$

II. EXPERIMENTAL

A. Sample preparation

The periodic doping structures in GaAs were grown by molecular-beam epitaxy in an UHV system of the vertical evaporation type equipped with a sample exchange load-lock system. The GaAs(100) semi-insulating substrate was kept at 530°C during growth. Hyperabrupt p - n junctions were achieved by using Si for n -type and Be for p -type doping and actuating the mechanical shutters in front of the dopant effusion cells in an appropriate way.^{16,18} The doping concentration was well adjusted by the intensity of the respective dopant molecular beam. For the present study a

total of 20 alternating n - and p -doped GaAs layers corresponding to 10 periods were deposited at a growth rate of 1 $\mu\text{m}/\text{h}$. No intrinsic layers were interspersed between. The first GaAs layer grown onto the substrate was always n doped; the final top layer always p doped. The thicknesses of the constituent layers were varied between 150 nm and 300 nm in different samples.

As an example, the properties of one representative periodic doping multilayer structure in GaAs will be discussed in this paper. The n and p layers of this sample (No. 2282) have the same thickness of $1.9 \times 10^3 \text{ \AA}$. The doping concentration in the n layers is $n_D = 3.0 \times 10^{17} \text{ cm}^{-3}$, whereas the concentration in the p layers is lower, $n_A = 1.9 \times 10^{17} \text{ cm}^{-3}$. The ground-state carrier concentration is

obtained from the expressions (20)–(24) with $\Delta\phi_{np}=0$, yielding $n^{(2)}(0)=2.5\times 10^{12}\text{ cm}^{-2}$ and $p^{(2)}(0)=4.2\times 10^{11}\text{ cm}^{-2}$.

The as-grown wafers were cleaved into rectangular pieces of about $0.3\text{--}0.4\text{ cm}^2$ area. Selective n^+ electrodes forming excellent Ohmic contacts to *all* n -type layers were achieved by carefully alloying small Sn balls. Selective p^+ electrodes for measurements in the p layers were formed by using Sn-Zn balls. The electrodes produced in this manner are selective as they form blocking p - n junctions with respect to the layers of opposite doping.

B. Experimental procedure

The sample was illuminated with monochromatic light obtained from a tungsten-iodine lamp by means of a Jarrel-Ash $\frac{1}{4}$ -m monochromator. The light was transmitted through a glass fiber into the cryostat onto the sample, held at 4.2 K. The electrical contacts on the sample were shielded against light with a mask leaving a central illuminated region of $4\times 10^{-2}\text{ cm}^2$. Typical light intensities through the mask on the sample were in the order of $10^2\text{--}10^{13}$ photons/sec cm^2 . Neutral-density filters were used to vary the photon flux.

The conductance G_{nn} (G_{pp}) of the n layers (p layers) parallel to the layers was determined with an automatic system connected to a desk-top calculator. The current between the two contacts was measured with high precision using a pA meter of high resolution (current range: $1\times 10^{-15}\text{--}2\times 10^{-2}\text{ A}$) attached to the calculator. The internal bias of the pA meter allowed us to deduce the conductance directly. Owing to the very short response time of the measuring system, the conductance as a function of time was recorded directly.

Figure 5 shows such a quasicontinuous electron-conductance versus time diagram $G_{nn}(t)$ of the doping multilayer sample. The diagram can be separated into three parts. For $t\leq t_1$ the conductance is constant and corresponds to the ground state of the sample ($\Delta\phi_{np}=0$) without optical excitation. The relatively high conductance of $3.8\times 10^{-3}\text{ }\Omega^{-1}$ in the n layers is due to the higher doping concentration and electron mobility as compared to the p layers. (The corresponding p -layer conductance is only $2.8\times 10^{-5}\text{ }\Omega^{-1}$.)

At $t=t_1$ the illumination of the sample by the monochromatic light of photon energy $\hbar\omega=1.473\text{ eV}$ and intensity $I_\omega=6\times 10^{12}$ photons/sec cm^2 is

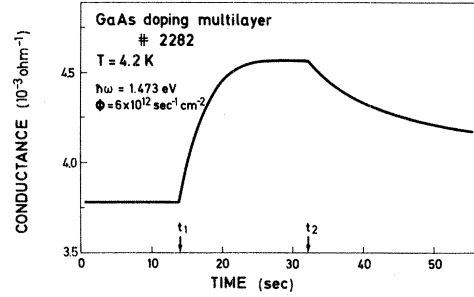


FIG. 5. Measured photoconductive response vs time of the GaAs np -doping multilayer structure used to calculate the absorption coefficient via Eqs. (40) and (40'). The photon flux $\Phi=6\times 10^{12}$ photons $\text{sec}^{-1}\text{ cm}^{-2}$ is switched on at $t=t_1$ and turned off at $t=t_2$.

switched on. An increase of the conductance with time is observed, which reflects the increasing free-carrier concentration due to electron-hole pair generation by absorption of photons, as described in Sec. I C.¹⁷ The slope of $G_{nn}(t)$ decreases continuously until $G_{nn}(t)$ becomes practically flat. A monotonous flattening due to both, decreasing absorption coefficient $\alpha^{\text{NIP1}}(\omega; \Delta\phi_{np})$ and increasing recombination rate $R(\Delta\phi_{np})$ is expected, according to our discussion in connection with the expression (40) in Sec. I C. The constant value of increased conductance is reached when the (decreasing) absorption rate per layer $\alpha^{\text{NIP1}}(\omega; \Delta\phi_{np}^{\text{max}})(I_\omega/\hbar\omega)d$ is balanced by the (increasing) recombination rate $R(\Delta\phi_{np}^{\text{max}})$.

After switching the light off at $t=t_2$ the optically induced conductance enhancement decays due to recombination of the excess charge carriers. The decay of the photoresponse, of course, is not an exponential one. The decrease slows down very soon, because of the decreasing recombination rate $R(\Delta\phi_{np})$ as $\Delta\phi_{np}$ becomes smaller. After 50 sec (the maximum time shown in Fig. 5), for example, the decrease by recombination

$\{ \dot{G}_{nn}(t)/[G_{nn}(t)-G_{nn}(t_1)] \}_{t=50\text{sec}} = -0.026\text{ sec}^{-1}$
is almost negligible against the corresponding increase by absorption

$\{ \dot{G}_{nn}(t)/[G_{nn}(t)-G_{nn}(t_1)] \}_{t=17\text{sec}} = 0.25\text{ sec}^{-1}$.

Assuming a constant electron mobility, one can convert $\dot{G}_{nn}(t)$ and $G_{nn}(t)$ into $\dot{n}^{(2)}(t)$ and $n^{(2)}(t)$ by

$$\dot{n}^{(2)}(t) = [\dot{G}_{nn}(t)/G_{nn}(t_1)]n^{(2)}(t_1) \quad (44)$$

and

$$n^{(2)}(t) = [G_{nn}(t)/G_{nn}(t_1)]n^{(2)}(t_1), \quad (45)$$

where $n^{(2)}(t_1)$ is the ground-state carrier concentra-

tion $n^{(2)}(\Delta\phi_{np}=0)=2.5\times 10^{12}\text{ cm}^{-2}$, given in Sec. II A. The dependence between $n^{(2)}$ and $\Delta\phi_{np}$, required for the determination of $\alpha(\omega;\Delta\phi_{np})$, finally, is obtained from the relation between $n^{(2)}$ and $\Delta\phi_{np}$ given by (20).

C. Results and discussion

The quantities $n^{(2)}(\Delta\phi_{np})$ and $R(\Delta\phi_{np})$ as deduced from the experimental conductance versus time curves taken during and after illumination at different photon energies were inserted into Eq. (40) in order to determine the absorption coefficient $\alpha(\omega;\Delta\phi_{np})$ as a function of frequency and potential difference $\Delta\phi_{np}$.

For a first comparison between theory and experiment we quote the ground-state absorption coefficient at $\Delta\phi_{np}=0$. $n^{(2)}(\Delta\phi_{np}=0)$ is deduced from the initial conductance increase at the time t_1 when the optical excitation starts. Conductance values are converted to the corresponding carrier concentration via Eqs. (44) and (45). Recombination is neglected since it is effectively suppressed at small $\Delta\phi_{np}$ values by the spatial separation of free electrons and holes by the space-charge potential barriers. For photon energies near $\hbar\omega=E_g^0$ the expression (40') is used instead of (40).

The photon-energy dependence of the ground-state absorption coefficient $\alpha^{\text{NIPi}}(\omega;\Delta\phi=0)$ determined in this way is shown in Fig. 6 (full squares). The theoretical curve (full line) is calculated with the design parameters n_D , n_A , d_n , and d_p of the sample, according to Sec. I B. Theory and experimental data fit well as far as the exponential decrease of α^{NIPi} below E_g^0 is concerned. The nearly frequency-independent shift of the experimental results to higher values of the absorption coefficient is attributed to systematic errors in the determination of I_ω which may be in the order of 50%. At absorption levels below 10^2 cm^{-1} even stronger deviations from theory occur. This behavior can be explained by additional absorption processes due to impurity levels as observed also in bulk material.¹⁹ The impurity related absorption is expected to be in the order of 10 cm^{-1} .

As an example of the modulation of the absorption coefficient by excitation we have evaluated $\alpha^{\text{NIPi}}(\omega;\Delta\phi_{np})$ for a Fermi-level splitting $\Delta\phi_{np}=0.45\text{ eV}$. The values of $G_{nn}(0.45\text{ eV})$ during optical excitation ($t_1 < t < t_2$) and after excitation ($t > t_2$) were used to deduce $n^{(2)}(0.45\text{ eV})$ and $R(0.45\text{ eV})$ and finally $\alpha^{\text{NIPi}}(\omega;0.45\text{ eV})$ via Eqs.

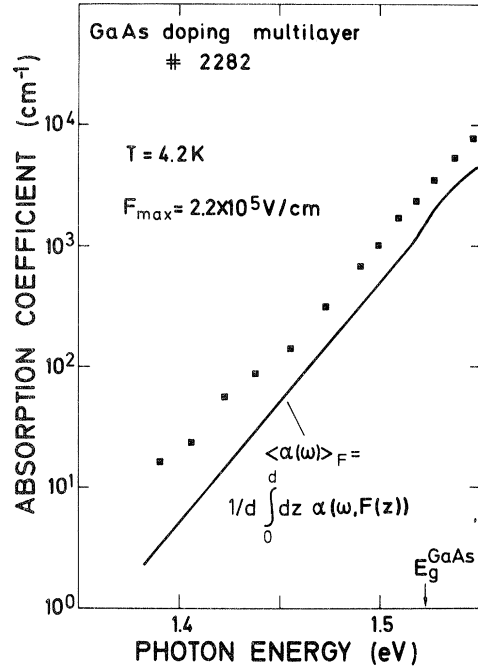


FIG. 6. Absorption coefficient in the ground state of a doping superlattice with $d_n=d_p=190\text{ nm}$, $n_D=3.0\times 10^{17}\text{ cm}^{-3}$, and $n_A=1.9\times 10^{17}\text{ cm}^{-3}$. Experimental points obtained from the photoconductive response. Theoretical curve calculated with the design parameters, using Eq. (32).

(40) and (40'). The values of $\alpha^{\text{NIPi}}(\omega;0.45\text{ eV})$ are, indeed, remarkably smaller as compared to the corresponding ground-state values at $\hbar\omega < E_g^0$ since the periodic space-charge potential flattens with increasing $\Delta\phi_{np}$ and so the internal electric fields are reduced.

In Fig. 7 the measured relative changes of the

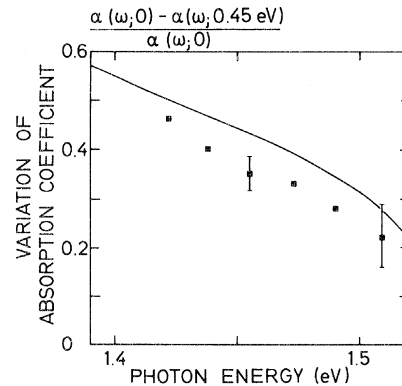


FIG. 7. Relative changes of the absorption coefficient induced by optically exciting the doping superlattice with design parameters as in Fig. 4. The excited state corresponds to a quasi-Fermi-level splitting $\Delta\phi_{np}=0.45\text{ eV}$. Open rectangles indicate experimental results, full line is calculated.

absorption coefficient between $eU_{np}=0.45$ eV and $eU_{np}=0$ eV are shown (squares). Also shown are the corresponding calculated changes (full line). Apparently there is good agreement between observed and theoretically expected tunability of the absorption coefficient.

The increase of the absorption coefficient at negative values of $\Delta\phi_{np}$ can be studied in a similar manner, if a negative external potential $eU_{np}=\Delta\phi_{np}<0$ is applied to the doping superstructure via selective electrodes as mentioned in Sec. I C.⁴ In this case $G_{nn}(t)$ is positive in the dark and under illumination as well. $\alpha^{\text{NIPi}}(\omega;\Delta\phi_{np})$, again, can be determined from the difference in $G_{nn}(t)$.

With selective electrodes on the sample it is also possible to modulate the absorption coefficient electrically by varying $\Delta\phi_{np}$ via an external bias U_{np} , as discussed in Sec. I C. In order to obtain sufficiently large changes in the transmitted light intensity, the product of change of absorption coefficient and effective sample thickness

$$[\alpha^{\text{NIPi}}(\omega;\Delta\phi_{np,2})-\alpha^{\text{NIPi}}(\omega;\Delta\phi_{np,1})]D^{\text{eff}}$$

may not be too small. Thus, transmission of the light parallel to the layers or multiple reflection of the beam is required for investigating the modulation of the absorption coefficient at photon energies far below E_g^0 .

So far we have deduced the absorption coefficient from the photoconductive response under the assumption that the collection probability for the electron-hole pairs is unity. Therefore, a comparison with $\alpha(\omega;\Delta\phi_{np})$ determined from transmission experiments would provide interesting information on the validity of this approximation. The results obtained in the present study indicate that the efficiency is rather close to unity, as the experimental absorption values are even higher than theoretically expected.

III. CONCLUDING REMARKS

We have demonstrated that the absorption coefficient of semiconductors with np -doping super-

structure ("NIPi" superlattice) is a tunable quantity and exhibits an exponential tail at photon energies below the gap of the unmodulated semiconductor, as predicted by theory. Both the measured frequency dependence and its variation upon modulation of the effective energy gap E_g^{NIPi} agree quantitatively with theory.

We plan to extend the measurements to lower photon energies and to larger variation of the effective energy gap, including negative changes by means of selective electrodes for electrons and holes, respectively. The possibility of varying the absorption coefficient by external bias applied to selective electrodes will be used also for a modulation of the transmitted light. This kind of study allows an independent alternative determination of the tunability and frequency dependence of the absorption coefficient. It is, however, also of considerable interest with respect to possible device applications.

Our theoretical treatment of absorption in NIPi crystals has been based on a simplified continuum model. Besides the quantum effects due to two-dimensional subband formation¹⁵ (which, indeed, are expected to be negligible for the samples with large superlattice period as investigated in this work) we have also neglected the effect of deviations from the effective-mass approximation and the polarization dependence of the absorption coefficient in the case of nonperpendicular incidence.

ACKNOWLEDGMENTS

We would like to thank A. Fischer for expert help in sample preparation, J. Knecht for contacting the multilayer samples, H. G. Fischer for technical assistance with the photoconductivity measurements, and B. Fischer for critical reading of the manuscript. Part of this work was supported by the Bundesministerium für Forschung und Technologie of the Federal Republic of Germany.

¹L. Esaki and R. Tsu, IBM J. Res. Develop. **14**, 61 (1970).

²For recent reviews and overviews, see, G. S. Sai-Halasz, in *Physics of Semiconductors—1978*, edited by B. L. Wilson (IOP, London, 1979), p. 21, and various

papers in Surf. Sci. **98**, 70 (1980).

³K. Ploog, A. Fischer, G. H. Döhler, and H. Künzel, in *GaAs and Related Compounds—1980*, edited by H. W. Thim (IOP, London, 1981), p. 721.

⁴K. Ploog, H. Künzel, J. Knecht, A. Fischer, and G. H.

- Döhler, Appl. Phys. Lett. 38, 870 (1981).
- ⁵G. H. Döhler, Phys. Status Solidi B 52, 79 and 533 (1972).
- ⁶G. H. Döhler, J. Vac. Sci. Technol. 16, 851 (1979).
- ⁷G. H. Döhler and K. Ploog, Prog. Crystal Growth Charact. 2, 145 (1979).
- ⁸This effect is similar to the persistent photoconductive response reported by H. J. Queisser and D. E. Theodore, Phys. Rev. Lett. 43, 401 (1979).
- ⁹G. H. Döhler, Surf. Sci. 73, 97 (1978).
- ¹⁰We are neglecting the fact that (17) and (18) are no longer correct if $n^{(2)}$ and/or $p^{(2)}$ approach zero. This restriction, however, concerns only the range of $\Delta\phi_{np} \lesssim \Delta\phi_{np}^{\text{th}}$.
- ¹¹G. H. Döhler, P. Ruden, H. Künzel, and K. Ploog (unpublished).
- ¹²W. Franz, Z. Naturforsch. 13, 484 (1958); L. V. Keldysh, Zh. Eksp. Teor. Fiz. 34, 1138 (1958) [Sov. Phys.—JETP 7, 788 (1958)].
- ¹³D. E. Aspnes and N. Bottka, in *Semiconductors and Semimetals*, edited by R. K. Willardson and A. C. Beer (Academic, New York, 1972), Vol. 9, p. 457.
- ¹⁴The constant C in (33) and (37) has been determined from the experimental absorption data for unmodulated bulk GaAs from Ref. 19.
- ¹⁵G. H. Döhler, H. Künzel, D. Olego, K. Ploog, P. Ruden, H. J. Stolz, and G. Abstreiter, Phys. Rev. Lett. 47, 864 (1981).
- ¹⁶H. Künzel, G. H. Döhler, and K. Ploog, Appl. Phys. A 27, 1 (1982).
- ¹⁷Note that the photon flux incident to the sample has to be related to the total cross section of the sample and not to the illuminated area, as the increase $n^{(2)}$ and $p^{(2)}$ is spread homogeneously over the whole sample.
- ¹⁸K. Ploog, A. Fischer, and H. Künzel, J. Electrochem. Soc. 128, 400 (1981).
- ¹⁹M. D. Sturge, Phys. Rev. 127, 768 (1962).